

# Uniaxial Alignment of Liquid-Crystalline Conjugated Polymers by Nanoconfinement

Zijian Zheng,<sup>‡,§</sup> Keng-Hoong Yim,<sup>||</sup> Mohammad S. M. Saifullah,<sup>†,§</sup>  
Mark E. Welland,<sup>§</sup> Richard H. Friend,<sup>\*,||</sup> Ji-Seon Kim,<sup>\*,||</sup> and Wilhelm T. S. Huck<sup>\*,‡,§</sup>

*Melville Laboratory for Polymer Synthesis, Department of Chemistry, University of Cambridge, Lensfield Road, Cambridge CB2 1EW, United Kingdom, The Nanoscience Centre, University of Cambridge, 11 J. J. Thomson Avenue, Cambridge CB3 0FF, United Kingdom, and Optoelectronics Group, Department of Physics, University of Cambridge, Madingley Road, Cambridge CB3 0HE, United Kingdom*

Received January 4, 2007; Revised Manuscript Received February 19, 2007

## ABSTRACT

We demonstrate the uniaxial alignment of a liquid-crystalline conjugated polymer, poly(9,9-dioctylfluorene-*co*-benzothiadiazole) (F8BT) by means of nanoconfinement during nanoimprinting. The orientation of the conjugated backbones was parallel to the nanolines imprinted into the polymer film. Polarized UV–vis absorption and photoluminescence spectra were measured to quantify the degree of alignment, showing that the polarization ratio and uniaxial molecular order parameter were as high as 66 and 0.97, respectively. The aligned F8BT film was used as the active layer in a PLED, which resulted in polarized electroluminescence with a polarization ratio of 11. Ambipolar PFET in a top-gate configuration with aligned F8BT as the active semiconducting layer showed mobility enhancement when the chains were aligned parallel to the transport direction. Mobility anisotropies for hole and electron transport were 10–15 and 5–7, respectively, for current flow parallel and perpendicular to the alignment direction.

Since the first report of electroluminescence (EL) of conjugated polymers by Burroughes et al.,<sup>1</sup> a wide range of optoelectronic devices including LEDs, FETs, and solar cells have been constructed from semiconducting polymers. Many of the most commonly used conjugated polymers such as substituted poly(*p*-phenylenevinylene) (PPV), poly(9,9-dioctylfluorene-*co*-benzothiadiazole) (F8BT), and poly(9,9-dioctylfluorene-*co*-bithiophene) (F8T2) have been found to exhibit thermotropic liquid-crystalline (LC) phases as a result of the stiff, conjugated backbone and the long alkyl side chains that are introduced to increase solubility.<sup>2–5</sup> LC polymers show a preference for alignment of chains into microscopic monodomains, and this has been exploited in the enhancement of the mobility of charges in polymer field effect transistors (PFETs)<sup>6</sup> and the fabrication of polymer light-emitting diodes (PLEDs) that emit polarized light.<sup>7</sup> To induce the alignment of chains over macroscopic distances into large area monodomains, an alignment layer is used,

typically consisting of a mechanically rubbed<sup>6,7</sup> or photo-aligned polyimide (PI).<sup>8</sup> Other aligning methods include: (1) stretching or rubbing the polymer films,<sup>9,10</sup> (2) Langmuir–Blodgett deposition,<sup>11</sup> (3) luminescent guest molecules in an aligned host matrix,<sup>12,13</sup> or (4) alignment with magnetic/electric field or photoirradiation.<sup>14–16</sup> In this paper, we present a method for aligning LC conjugated polymers into macroscopic monodomains by nanoconfining the polymers in one-dimensional nanochannel arrays using nanoimprinting.<sup>17–20</sup> This approach is based on the recent observation by Yang et al.<sup>21</sup> who reported the formation of nonspherical polymer colloids by nanoconfining main-chain LC polymers into volumes with dimensions far smaller than the LC domain size. By fabricating molds for nanoimprinting with feature dimensions much smaller than the size of typical monodomains, we can force the LC polymers to align along the walls of the features, thereby aligning the chains over macroscopic distances. Kim et al. reported<sup>22</sup> the alignment of liquid-crystal small molecules with an imprinted polymer layer for applications in liquid-crystal displays. However, this additive alignment layer is not desirable in PLEDs architecture. In contrast, imprinting semiconducting, light-emitting LC polymers allows the fabrication of PLEDs emitting polarized light without any additive layer. Opposite

\* Corresponding author. E-mail: rhf10@cam.ac.uk (R.H.F.); jsk20@cam.ac.uk (J.-S.K.); wtsh2@cam.ac.uk (W.T.S.H.).

† Current address: Opto- and Electronic Systems Cluster, Institute of Materials Research and Engineering, 3 Research Link, Singapore 117602, Singapore.

‡ Melville Laboratory for Polymer Synthesis.

§ The Nanoscience Centre.

|| Optoelectronics Group, Department of Physics.

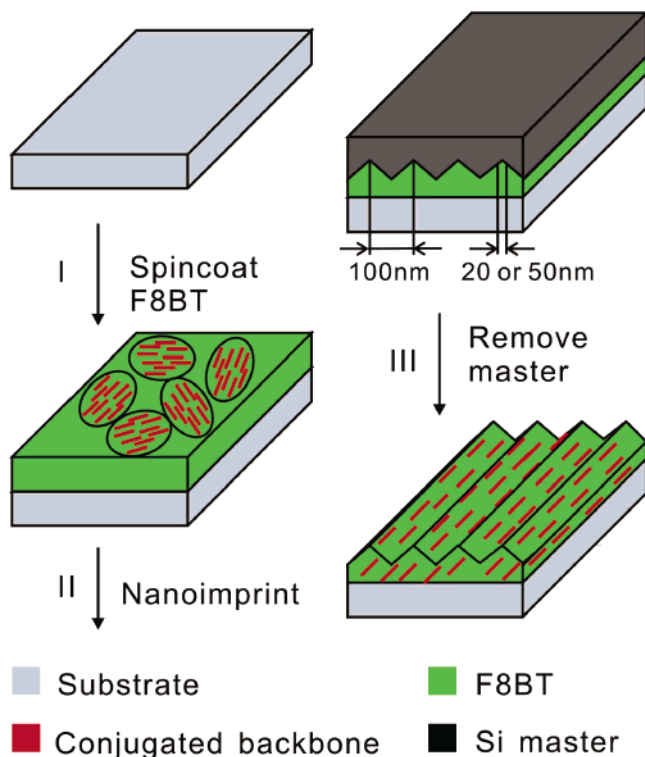


**Figure 1.** Schematic process of aligning F8BT by nanoconfinement.

to the traditional bottom-up alignment on polymer/substrate interface,<sup>6–8,22</sup> our top-down approach produces the best anisotropy on the mold/polymer interface, which can more effectively enhance charge carrier mobilities in PFETs in a bottom-contact/top-gate configuration.

In this study, a green-emitting LC polymer, F8BT, was chosen because it is relatively stable in air and its physical properties have been studied in detail.<sup>23</sup> The alignment process is schematically shown in Figure 1: first, films were prepared by spincoating a *p*-xylene solution of F8BT ( $M_n \sim 9000$ ,  $T_g \sim 90$  °C) on precleaned substrates (quartz, silicon wafer, or ITO on glass). The film thickness was varied according to solution concentration and spin speed. A silicon mold (previously coated with a nonadhesive layer) of nanochannel arrays was placed against the F8BT film. Subsequently, this assembly was put into an Obducat nanoimprinter (Obducat AB, Sweden) and imprinted at 160 °C and 40 bar for 5 min, then allowed to cool down to 70 °C before releasing the pressure. During this process, F8BT flowed into the nanochannels at temperatures above the  $T_g$ ;<sup>23</sup> when cooled down to temperatures below  $T_g$ , all polymer chains were “frozen” and therefore the alignment remained. Finally, a macroscopically monodomain-aligned F8BT film was obtained after removing the mold. The degree of alignment was evaluated by polarized UV–vis absorbance, polarized photoluminescence (PL), and polarized EL measurements, all indicating a high degree of order at the molecular level as shown later in the paper.

We visualized the nanoimprinting quality by scanning electron microscopy (SEM). As shown in Figure 2a and b, the patterns of the Si molds are 20 nm × 80 nm (20 nm

nanochannels with an 80 nm gap) and 50 nm × 50 nm. These molds were fabricated by electron-beam lithography followed by reactive ion etching (RIE) and coated with a self-assembled monolayer of 1*H*,1*H*,2*H*,2*H*-perfluorodecyltrichlorosilane (FluoroChem) as a nonadhesive layer. Parts c and d of Figure 2 show SEM images of imprinted F8BT, which follow the complementary patterns of their corresponding mold nicely over very large areas (1 cm<sup>2</sup>). It should be noted that the 20 nm × 80 nm F8BT pattern shows a zigzag surface topography (Figure 2c, inset), which is due to the isotropic etching of the Si mold. These F8BT lines are about 25 nm in height and the total film thickness is  $\sim 70$  nm.

The degree of alignment was first quantified by polarized UV–vis absorption measurements. A 70 nm F8BT film was deposited on quartz by spin-coating a 2.4 wt % F8BT solution at 3000 rpm for 60 s. The film was aligned with the 20 nm × 80 nm mold as described above and placed in a HP8453 UV–vis spectrometer (Hewlett-Packard) in which incident light was filtered by a polarizer. As shown in Figure 3a, aligned F8BT had the strongest absorption when the polarization of incident light was parallel (||) to the nanolines and the weakest when it was perpendicular ( $\perp$ ). The dichroic ratio  $D = A_{||}/A_{\perp}$  is 7 in the spectral region of the F8BT  $\pi$ – $\pi^*$  transition (460 nm). By rotating the polarizer, the absorption of the aligned F8BT appeared sinusoidal, with a periodicity of 180°.

We also measured the polarized photoluminescence (PL) spectra of the aligned F8BT. The same sample was fixed on a rotator on a normal optical microscope and irradiated with blue excitation through a polarizer. The green light emitted by F8BT passed through an analyzer, and the resultant fluorescence was recorded using a grating spectrograph connected to an Oriel Instaspec IV CCD array with an optical fiber. As shown in Figure 3b, the strongest luminescence was recorded when both polarizations of polarizer and analyzer were parallel to the nanochannels. In contrast, when they were perpendicular to the nanolines, the lowest luminescence was observed. The polarization ratio  $P = I_{||}/I_{\perp}$  is about 12 at 540 nm, which corresponds to a uniaxial molecular order parameter  $R$  of 0.85, given that  $R = (I_{||} - I_{\perp})/(I_{||} + 2I_{\perp})$ . The degree of alignment can be enhanced by either decreasing the film thickness or extending the imprinting time (Figure 3c). We found the best results for films below 30 nm thickness and imprinted for 1 h (or 5 min at higher temperatures). For example,  $P$  and  $R$  of a 27 nm F8BT film imprinted at 160 °C, 40 bar for 60 min are as high as 66 and 0.97, respectively.

There are two possible mechanisms for the chain alignment: polymer crystal ordering or self-organization in liquid-crystalline phase. For this first possibility, Hu and Jonas<sup>17</sup> have reported that the orientation of polymer crystals can be fully controlled at the nanoscale by using nanoimprint lithography. In their case, thin films of poly(vinylidene fluoride) (PVDF) crystallized in the nanoconfinement during imprinting, resulting in crystal ordering. However, the *c*-axis (backbone) of PVDF was normal to the substrate, and the ordering was very low when the film thickness was larger than the depth of the mold. In contrast, the backbone of F8BT

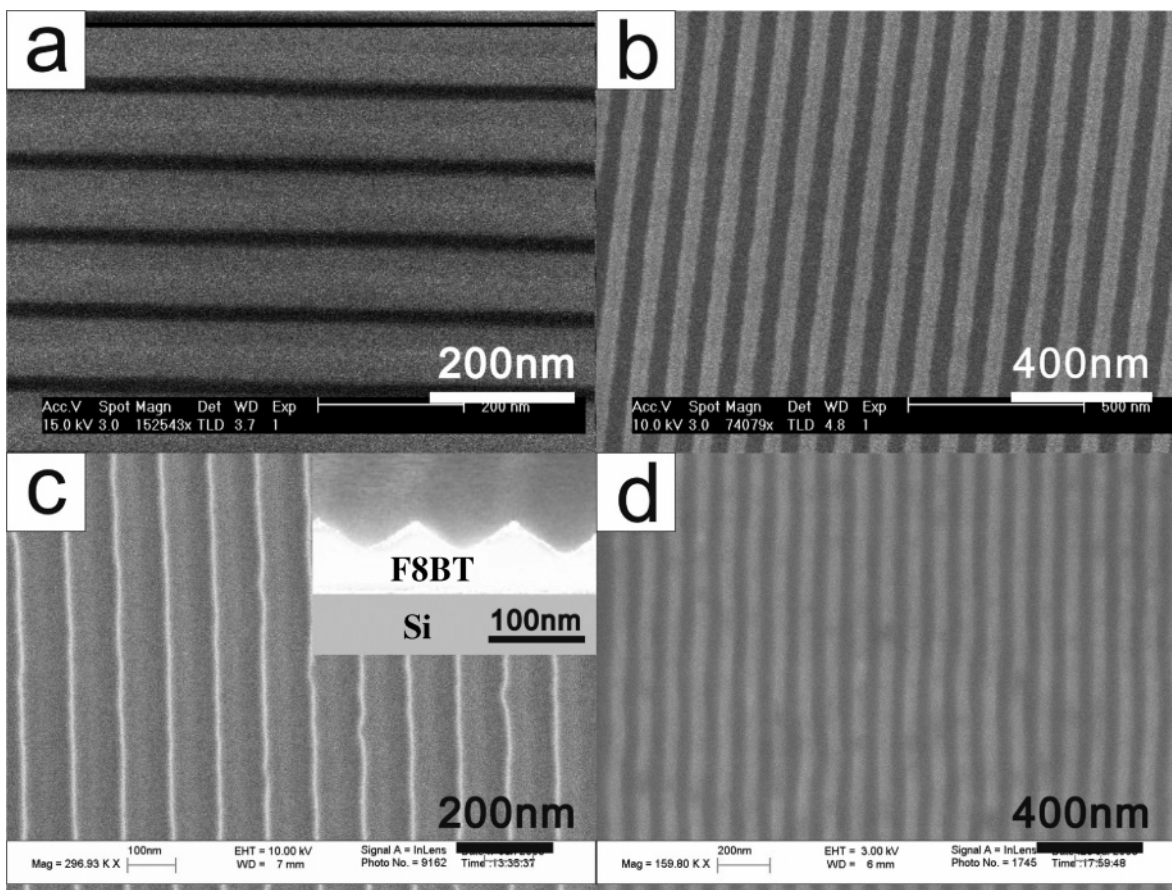


**Figure 2.** SEM images of (a) 20 nm × 80 nm Si mold, (b) 50 nm × 50 nm Si mold, (c) imprinted F8BT using mold (a), inset shows its surface topography, and (d) imprinted F8BT using mold (b).

is aligned parallel to the substrate, and we observed very high ordering even with film thicknesses about 3 times of the depth of the features on the mold. The second possibility is that nanoconfinement resulted in a significant depression of the liquid-crystalline transition temperature of F8BT. It is well-known that the  $T_g$  of polymers in thin films is different from the bulk value, with large deviations for films under 30 nm,<sup>24–28</sup> as well as a strong dependency on surface energy, with further decreases of the  $T_g$  for low interfacial energies at the polymer/substrate interface.<sup>28</sup> Mundra et al.<sup>29</sup> also reported very recently that the  $T_g$  can be further decreased by introducing 1D nanostructures on polymer thin films. Therefore, it is very likely that the F8BT reached its nematic phase at 160 °C even though the transition ( $T_{Nbulk}$ ) occurs at 195 °C in bulk.<sup>23</sup> The presence of the nanoscale trenches on the perfluorinated molds then ordered the chains into macroscopically sized LC monodomains. The high polarization ratios and order parameters strongly suggest that all polymer chains in the thin film are aligned. However, because the total thickness of aligned films (up to 70 nm) can be 3 times the height of relief structures (25 nm), we believe that the polymer layer underneath the nanolines (thus not nanoconfined in the nanochannels) was also aligned, which must be due to the larger scale self-organization of the LC polymer chains directed by the nanostructured surface. This effect obviously becomes weaker in thicker films (Figure 3c).

One may ask whether the nanopattern affects the polarization of the emitted/absorbed light. To rule out this argument, we imprinted the same mold (20 nm × 80 nm) into a 70 nm thick poly(2,7-(9,9-di-*n*-octylfluorene)-*alt*-(1,4-phenylene-((4-sec-butylphenyl)imino)-1,4-phenylene)) (TFB) film, which is an amorphous polymer because the phenyl amine groups disrupt any packing of the chains. In previous experiments, nanoparticles of TFB showed no preferential ellipsoidal shape.<sup>21</sup> The patterned TFB film showed no polarization in polarized UV–vis absorption (Figure 3d) and was black under cross polarizers (not shown). We therefore conclude that the nanopattern itself does not lead to polarization of transmitted light and that it is the uniaxial alignment of the F8BT chains due to nanoconfinement imposed in the imprinting process.

This method can be applied to align any LC polymer film in its LC phase on most substrates without an alignment layer or external electric/magnetic field. Therefore, it would be very suitable for preparing uniaxial films for polymer electronics requiring anisotropic properties in the active layer such as polarized PLEDs for backlights of liquid-crystal displays. The PLED was fabricated as follows: 70 nm F8BT was spin-coated on a PEDOT/PSS-covered ITO/glass substrate and aligned as describe above. Then a thin layer of Ca(20 nm)/Al(100 nm) was thermally evaporated on to the aligned F8BT through a mask, followed by encapsulation.

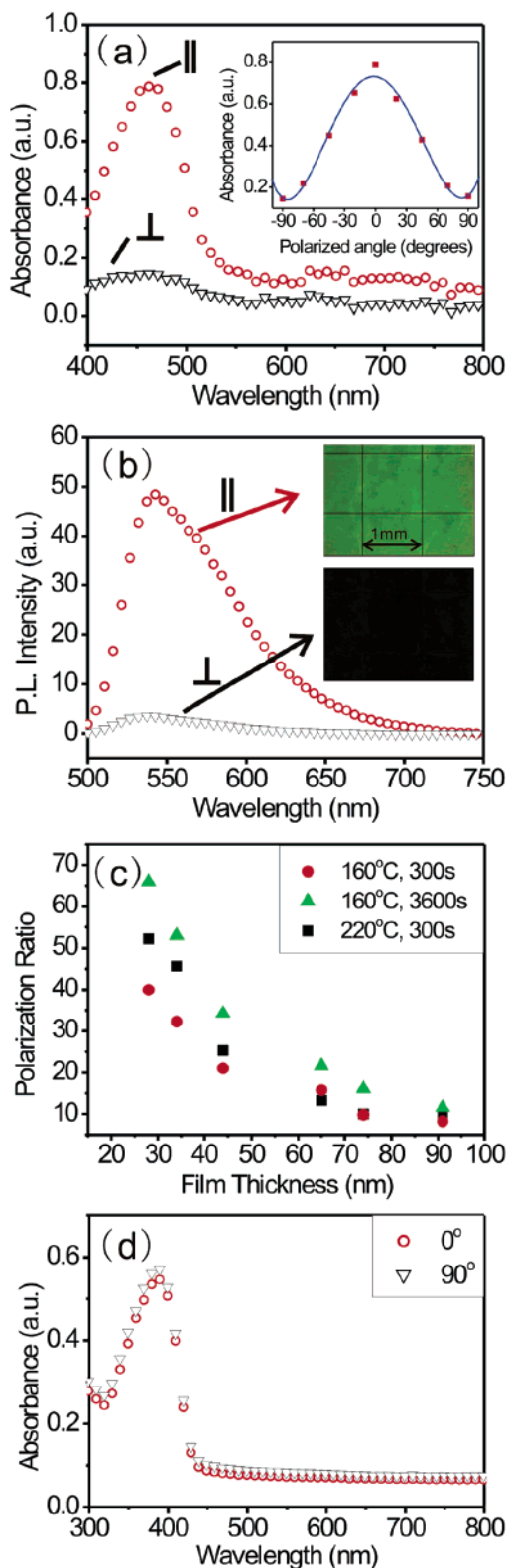


**Figure 3.** (a) Polarized UV-vis absorption spectra of aligned F8BT. The inset shows absorption peak intensity at different polarized angles. (b) Polarized PL spectra of aligned F8BT. The insets show the corresponding PL images. (c) Polarization ratio calculated from polarized PL measurements at different film thickness and imprinting time. F8BT films were imprinted at 160 °C for 300 s (●) or 3600 s (▲) and 200 °C for 300 s (■). (d) Polarized UV-vis absorption spectra of imprinted TFB. In spectra a, b, and d, polarization of polarizer is parallel (empty circle) and perpendicular (empty triangle) to the direction of nanolines.

A polarizer was fixed in between the device's forward direction and the spectrometer for polarized EL measurements. The device turned on at  $\sim 3$  V and polarized EL was recorded at 7 V (because no rubbed PI layer is required to align the chains, the devices do not require high driving voltages). The EL emission appears green, with an emission maximum at 540 nm. As shown in Figure 4a, we recorded the highest EL when the polarization of polarizers was parallel to the alignment direction and the largest polarization ratio is  $\sim 11$  at 540 nm. Figure 4b shows the optical images of EL when the polarization angle between polarizer and alignment direction was  $0^\circ$ ,  $45^\circ$ , and  $90^\circ$ .

We also demonstrate the applicability of this method to enhance charge carrier mobilities in PFETs. Previously, Siringhaus et al.<sup>6</sup> reported the enhancement of hole mobilities by aligning a LC semiconductor on a rubbed PI layer in a bottom-contact/top-gate configuration PFET in which the molecules aligned best at the semiconductor/PI interface. However, the best alignment should ideally be at the semiconductor/dielectric interface where the channel is formed, which can be directly achieved by our top-down approach. Our top-gate PFET<sup>30</sup> consists of F8BT ( $\sim 50$  nm) spun on glass substrates with prepatterned gold electrodes (by photolithography,  $L = 20 \mu\text{m}$ ,  $W/L = 500$ ), and aligned at 160 °C for 5 min. Poly(methyl methacrylate) (PMMA,  $M_n = 1\,200\,000$ , Aldrich), 500 nm thick, was then spun on top of the aligned F8BT, followed by thermal evaporation of a gold gate electrode. PFETs with either pristine F8BT and or F8BT film imprinted with a flat Si mold at the same condition as the active semiconducting layer were also fabricated for comparison. All devices showed ambipolar characteristics (Supporting Information, SI), when a dielectric layer not containing electron-trapping groups was used, such as PMMA.<sup>30</sup> Saturation mobilities of holes and electrons were calculated after correcting the actual device dimensions at the F8BT/PMMA interface introduced by the nanoimprinting process and are summarized in Table 1. Both PFETs with pristine and annealed (with flat Si mold) F8BT films show a similar hole ( $4\text{--}6 \times 10^{-4} \text{ cm}^2 \text{ V}^{-1} \text{ s}^{-1}$ ) and electron ( $1\text{--}2 \times 10^{-4} \text{ cm}^2 \text{ V}^{-1} \text{ s}^{-1}$ ) mobilities, indicating insignificant degradation of F8BT films in the imprinting process at elevated temperature. Compared to pristine F8BT, both carrier mobilities were enhanced when polymer chains were aligned parallel to the transport direction, as evident in Table 1. The hole mobility anisotropy for current flow parallel and perpendicular to the alignment direction ( $\mu_{H\parallel}/\mu_{H\perp} = 10\text{--}15$ ) is higher than that of electron mobility ( $\mu_{E\parallel}/\mu_{E\perp} = 5\text{--}7$ ), which we attribute to different transport mechanisms of these carriers in F8BT films. Quantum chemical calculations revealed strong localization of electrons on the BT unit in the lowest unoccupied molecular orbital (LUMO) of F8BT, whereas holes are delocalized along the polymer backbone in the highest occupied molecular orbital (HOMO).<sup>31</sup> When chains are aligned in the transport direction, hole transport along the conjugated segments of the polymer backbone is significantly faster than interchain hopping between adjacent chains, hence the high mobility anisotropy. In contrast, intrachain electron transport in F8BT is not a very efficient

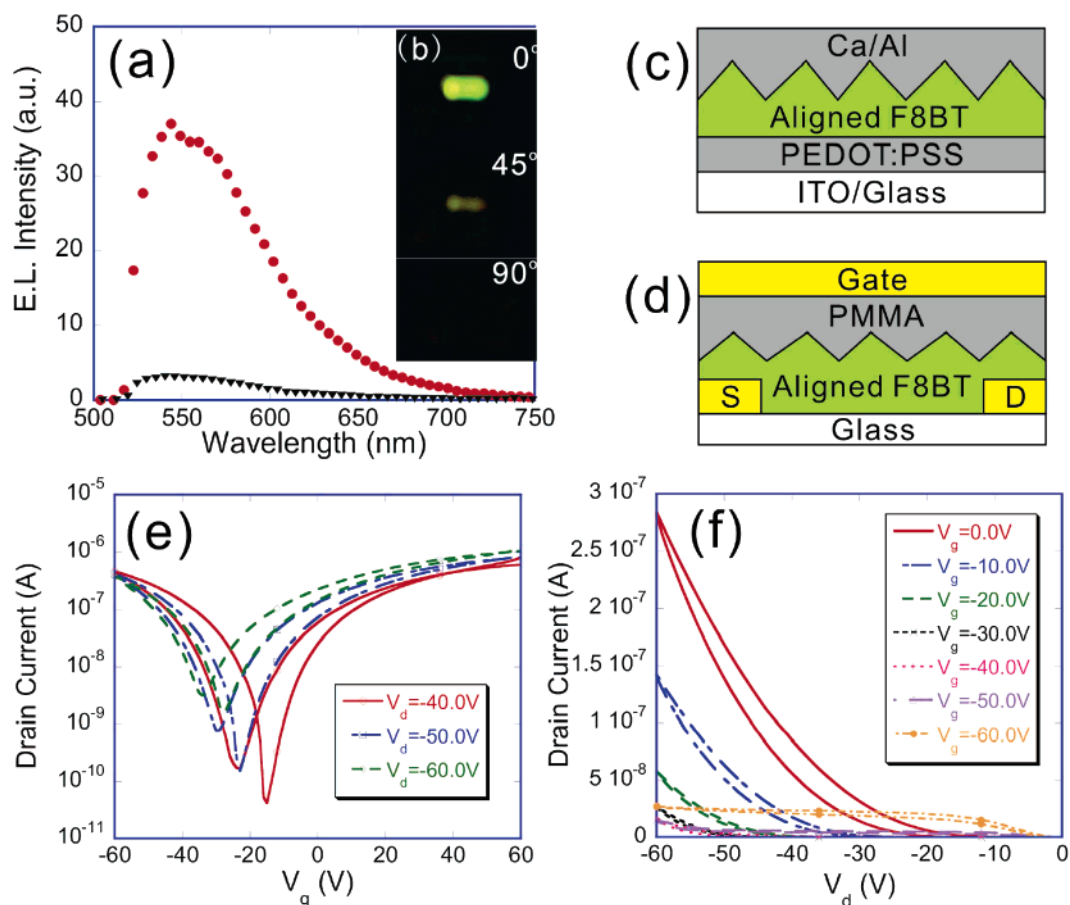


**Figure 4.** (a) EL measurement of PLED with an aligned F8BT active layer. Polarization of polarizer is parallel (circle) and perpendicular (triangle) to the alignment direction. (b) Optical images of EL at different polarized angle of polarizer. The pixel size is  $1.5 \times 3 \text{ mm}^2$ . (c) PLED device structure. (d) PFET device structure using gold as electrodes. (e) Transfer characteristics of an aligned ambipolar F8BT transistor. (f) Output characteristics of an aligned ambipolar F8BT transistor.

**Table 1.** Summary of Carrier Mobilities of PFETs with (un)Aligned F8BT as the Active Semiconducting Layer

	$\mu_{\text{pristine}} (\text{cm}^2 \text{V}^{-1} \text{s}^{-1})$	$\mu_{\text{flatmold}} (\text{cm}^2 \text{V}^{-1} \text{s}^{-1})$	$\mu_{\parallel} (\text{cm}^2 \text{V}^{-1} \text{s}^{-1})$	$\mu_{\perp} (\text{cm}^2 \text{V}^{-1} \text{s}^{-1})$	$\mu_{\parallel}/\mu_{\perp}$
hole mobility	$4-6 \times 10^{-4}$	$4-6 \times 10^{-4}$	$8-12 \times 10^{-4}$	$5-8 \times 10^{-5}$	10–15
electron mobility	$1-2 \times 10^{-4}$	$1-2 \times 10^{-4}$	$2-3 \times 10^{-4}$	$3-5 \times 10^{-5}$	5–7

process due to the high-energy barrier of F8 sites sandwiched between BT sites, and hence a smaller anisotropy in electron mobility.

In conclusion, we demonstrated the uniaxial alignment of liquid-crystalline conjugated polymer (F8BT) films by means of nanoconfinement using a nanoimprinting process. The orientation of conjugated backbones was parallel to the structures imprinted into the polymer film and parallel to the substrate. Polarized UV–vis absorption and PL were measured to quantify the degree of alignment. The results showed F8BT was better aligned when the film was thinner or imprinting time was longer. The polarization ratio  $P$  and uniaxial molecular order parameter  $R$  were recorded as high as 66 and 0.97, respectively. The aligned F8BT film was used as the active layer in PLED devices, which yielded an EL polarization ratio of 11. PFETs with 50 nm aligned F8BT as semiconductor showed ambipolar characteristics and mobility enhancement when the current flow direction was parallel to the alignment direction. Taking the imprinting-

induced topography in the F8BT/PMMA interface into account, the anisotropy of hole and electron mobility is 10–15 and 5–7, respectively. This alignment method should be able to introduce order in a wide range of stiff, (liquid) crystalline semiconducting polymers and as such improve device performance in PLEDs and PFETs.

**Acknowledgment.** We thank the IRC in Nanotechnology, Dorothy Hodgkin Postgraduate Awards (Z.Z.) and Cambridge Display Technology Ltd. (CDT) for materials and financial support (Z.Z. and K.H.Y.). We thank D. Anderson and Dr. G. A. C. Jones for assistance with e-beam lithography and Prof. E. Terentjev for advice on liquid-crystalline polymers.

**Supporting Information Available:** Calculation details of mobility correction for the imprinting-induced topography. This material is available free of charge via the Internet at <http://pubs.acs.org>.

## References

- (1) Burroughes, J. H.; Bradley, D. D. C.; Brown, A. R.; Marks, R. N.; Mackay, K.; Friend, H. R.; Burn, P. L.; Holmes, A. B. *Nature* **1990**, *347*, 539.
- (2) Neher, D. *Adv. Mater.* **1995**, *7*, 691.
- (3) Bao, Z.; Chen, Y.; Cai, R.; Yu, L. *Macromolecules* **1993**, *26*, 5281.
- (4) Liem, H.-M.; Etchegoin, P.; Whitehead, K. S.; Bradley, D. D. C. *Adv. Funct. Mater.* **2003**, *13*, 66.
- (5) Grell, M.; Redecker, M.; Whitehead, K. S.; Bradley, D. D. C.; Inbasekaran, M.; Woo, E. P.; Wu, W.; Wu, W. *Liq. Cryst.* **1999**, *26*, 1403.
- (6) Sirringhaus, H.; Wilson, R. J.; Friend, R. H.; Inbasekaran, M.; Wu, W.; Woo, E. P.; Grell, M.; Bradley, D. D. C. *Appl. Phys. Lett.* **2000**, *77*, 406.
- (7) Grell, M.; Knoll, W.; Lupo, D.; Meisel, A.; Miteva, T.; Neher, D.; Nothofer, H.-G.; Scherf, U.; Yasuda, A. *Adv. Mater.* **1999**, *11*, 671.
- (8) Sakamoto, K.; Usami, K.; Uehara, Y.; Ushioda, S. *Appl. Phys. Lett.* **2005**, *87*, 211910.
- (9) Dyreklev, P.; Berggren, M.; Inganäs, O.; Andersson, M. R.; Wennerström, O.; Hjertberg, T. *Adv. Mater.* **1995**, *7*, 43.
- (10) Hamaguchi, M.; Yoshino, K. *Appl. Phys. Lett.* **1995**, *67*, 3381.
- (11) Cimrová, V.; Remmers, M.; Neher, D.; Wegner, G. *Adv. Mater.* **1996**, *8*, 146.
- (12) Hagler, T. W.; Pakbaz, K.; Voss, K. F.; Heeger, A. J. *Phys. Rev. B* **1991**, *44*, 8652.
- (13) Bastiaansen, C.; Schmidt, H.-W.; Nishino, T.; Smith, P. *Polymer* **1993**, *34*, 3951.
- (14) Shklyarevskiy, I. O.; Jonkheijm, P.; Stutzmann, N.; Wasserberg, D.; Wondergem, H. J.; Christianen, P. C. M.; Schenning, A. P. H.; Leeuw, D. M.; Tomović, Z.; Wu, J.; Müllen, K.; Mann, J. C. *J. Am. Chem. Soc.* **2005**, *127*, 16233.
- (15) Xu, Z.-S.; Lemieux, R. P.; Natansohn, A. *Chem. Mater.* **1998**, *10*, 3269.
- (16) Jin, S.-H.; Seo, H.-U.; Nam, D.-H.; Shin, W. S.; Choi, J.-H.; Yoon, U. C.; Lee, J.-W.; Song, J.-G.; Shin, D.-M.; Gal, Y.-S. *J. Mater. Chem.* **2005**, *15*, 5029.
- (17) Hu, Z.; Baralia, G.; Bayot, V.; Gohy, J.-F.; Jonas, A. M. *Nano Lett.* **2005**, *5*, 1738.
- (18) Chou, S. Y.; Krauss, P. R.; Renstrom, P. J. *J. Vac. Sci. Technol., B* **1996**, *14*, 4129.
- (19) Austin, M. D.; Chou, S. Y. *Nano Lett.* **2003**, *3*, 1687.
- (20) Ge, H.; Wu, W.; Li, Z.; Jung, G.-Y.; Olynick, D.; Chen, Y.; Liddle, J. A.; Wang, S.-Y.; Williams, R. S. *Nano Lett.* **2005**, *5*, 179.
- (21) Yang, Z.; Huck, W. T. S.; Clarke, S. M.; Tajbakhsh, A. R.; Terentjev, E. M. *Nat. Mater.* **2005**, *4*, 486.
- (22) Kim, Y.-T.; Hwang, S.; Hong, J.-H.; Lee, S. D. *Appl. Phys. Lett.* **2006**, *89*, 173506.
- (23) Donley, C. L.; Zaumseil, J.; Andreasen, J. W.; Nielsen, M. M.; Sirringhaus, H.; Friend, R. H.; Kim, J.-S. *J. Am. Chem. Soc.* **2005**, *127*, 12890.
- (24) Keddie, J. L.; Jones, R. A. L.; Cory, R. A. *Europhys. Lett.* **1994**, *27*, 59.
- (25) Kim, J. H.; Jang, J.; Zin, W.-C. *Langmuir* **2001**, *17*, 2703.
- (26) Soles, C. L.; Douglas, J. F.; Wu, W.-L.; Peng, H.; Gidley, D. W. *Macromolecules* **2004**, *37*, 2890.
- (27) Ellison, C. J.; Torkelson, J. M. *Nat. Mater.* **2003**, *2*, 695.
- (28) Fryer, D. S.; Peters, R. D.; Kim, E. J.; Tomasewski, J. E.; Pablo, J. J.; Nealey, P. F.; White, C. C.; Wu, W.-L. *Macromolecules* **2001**, *34*, 5627.
- (29) Mundra, M. K.; Konthu, S. K.; Dravid, V. P.; Torkelson, J. M. *Nano Lett.* **2007**, <http://dx.doi.org/10.1021/nl062894c>.
- (30) Zaumseil, J.; Donley, C. L.; Kim, J.-S.; Friend, R. H.; Sirringhaus, H. *Adv. Mater.* **2006**, *18*, 2708.
- (31) Cornil, J.; Gueli, I.; Dkhissi, A.; Sancho-Garcia, J. C.; Hennebicq, E.; Calbert, J. P.; Lemaire, V.; Beljonne, D.; Bredas, J. L. *J. Chem. Phys.* **2003**, *118*, 6615.

NL070022K